

# Size-Selective Urea-Containing Metal–Organic Frameworks as Receptors for Anions

Leili Esrafil, Ali Morsali,\* Mao-Lin Hu,\* Alireza Azhdari Tehrani, Lucia Carlucci, Pierluigi Mercandelli, and Davide M. Proserpio



Cite This: <https://dx.doi.org/10.1021/acs.inorgchem.0c02215>



Read Online

ACCESS |



Metrics & More

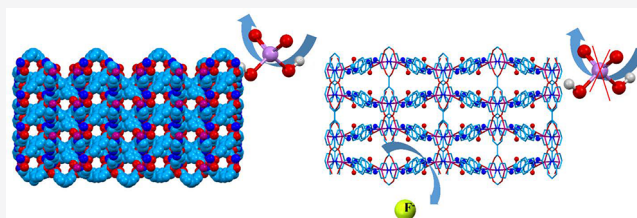


Article Recommendations



Supporting Information

**ABSTRACT:** Anion recognition by neutral hosts that function in aqueous solution is an emerging area of interest in supramolecular chemistry. The design of neutral architectures for anion recognition still remains a challenge. Among neutral anion receptor systems, urea and its derivatives are considered as “privileged groups” in supramolecular anion recognition, since they have two proximate polarized N–H bonds exploitable for anion recognition. Despite promising advancements in urea-based structures, the strong hydrogen bond drives detrimental self-association. Therefore, immobilizing urea fragments onto the rigid structures of a metal–organic framework (MOF) would prevent this self-association and promote hydrogen-bond-accepting substrate recognition. With this aim, we have synthesized two new urea-containing metal–organic frameworks, namely  $[Zn(bpdc)(L2)]_n \cdot nDMF$  (TMU-67) and  $[Zn_2(bdc)_2(L2)_2]_n \cdot 2nDMF$  (TMU-68) (bpdc = biphenyl-4,4'-dicarboxylate; bdc = terephthalate; L2 = 1,3-bis(pyridin-4-yl)urea), and we have assessed their recognition ability toward different anions in water. The two MOFs show good water stability and anion affinity, with a particular selectivity toward dihydrogen arsenate for TMU-67 and toward fluoride for TMU-68. Crystal structure characterizations reveal 3-fold and 2-fold interpenetrated 3D networks for TMU-67 and TMU-68, respectively, where all single interpenetrated networks are hydrogen bonded to each other in both cases. Despite the absence of self-quenching, the N–H urea bonds are tightly hydrogen bonded to the oxygen atoms of the dicarboxylate ligands and cannot be directly involved in the recognition process. The good performance in anion sensing and selectivity of the two MOFs can be ascribed to the network interpenetration that, shaping the void, creates monodimensional channels, decorated by exposed oxygen atom sites selective for arsenate sensing in TMU-67 and isolated cavities, covered by phenyl groups selective for fluoride recognition in TMU-68.



## 1. INTRODUCTION

Decades of research have been devoted to the discovery of new receptors for anion recognition and separation, due to the important role of anionic species in biological, environmental, and chemical processes.<sup>1,2</sup> This remains, however, an ongoing challenge, given some intrinsic properties of anions such as their largely variable size and shape, their high free energy of hydration, and the dependence of their nature on pH, which make their recognition in water quite different and more difficult with respect to that of metal cations.

Nature is the master key of anion recognition, and proteins are neutral receptors whose high selectivity is mainly due to noncovalent interactions, especially to hydrogen bonds.<sup>3,4</sup> The design and synthesis of anion receptors inspired by nature and based on specific noncovalent interactions are of central importance in supramolecular chemistry, attracting considerable attention from the scientific community and posing great challenges.<sup>5,6</sup>

Selective anion recognition can be achieved by both neutral and positively charged hosts. Cationic charged hosts are, undoubtedly, the primary approach but, as the recognition process is based on nondirectional electrostatic interactions,

they ensure poor anion selectivity, which is their main disadvantage.<sup>7,8</sup> On the other hand, neutral hosts with directional supramolecular interaction sites, such as hydrogen bonds, are unable to operate properly in a polar solvent such as water. Therefore, the design of neutral hosts as selective anion receptors able to work properly in aqueous solution is of great interest. An ideal neutral receptor possesses multiple strong hydrogen-bond-donor sites (such as urea, thiourea, amide, and pyrrole groups) in order to selectively bind their target anions. This class of anion receptors and their applicability have been well studied and documented.<sup>9,10</sup>

The emergence of metal–organic frameworks (MOFs) is one of the most essential events in coordination chemistry and materials science,<sup>11</sup> owing to their unique properties and extensive applications in many fields, including gas storage,<sup>12</sup>

Received: July 28, 2020

catalysis,<sup>13,14</sup> and sensing.<sup>15–18</sup> A great opportunity in MOF chemistry is the possibility of achieving predictable structures/topologies and porosities through a rational design process and chemical modification. Hydrophilic water-stable MOFs with hydrogen-bond-donating ability play an important role in applications such as biomedical technologies, water cleaning, and heat transformation because they are prone to self-assembly and consequently self-quenching.<sup>19–22</sup> “Self-quenching” here is defined as unproductive self-assembly behavior due to catalyst–catalyst interactions (e.g., dimerization, oligomerization, etc.). However, the design of these MOFs has encountered many challenges: (1) the majority of the reported MOFs cannot be directly used in applications that require exposure to water, as they are not stable with respect to the hydrolysis of metal and organic linkers, and (2) some of the MOFs incorporating hydrogen-bond-donating groups, such as thiourea, do not have thermal and chemical stability and have expensive and unstable ligands.<sup>23–27</sup> These challenges notwithstanding, it has been shown that incorporating supramolecular recognition sites into the MOF backbone has enabled the docking of a specific guest.<sup>27</sup> The pioneering work of Farha, Hupp, Scheidt and co-workers showed that incorporating urea groups into the MOF backbone gives an appropriate biomimetic alternative to Lewis acid activation.<sup>28</sup> Currently, urea-, thiourea-, and squaramide-containing metal–organic frameworks are in the spotlight due to their potential use as promising directional hydrogen-bond-donating homogeneous catalysts.<sup>29–32</sup> Indeed, the concepts of anion recognition and binding are critical factors for designing new organocatalysts, and the principles governing these recognition events can play a key role in the development of artificial enzymes in biological processes.<sup>33</sup>

Herein, we introduce two new urea-containing metal–organic frameworks as novel anion receptors. In these structures the urea moieties are not directly available for the recognition process, since they are involved in hydrogen bonding with the oxygen atoms of dicarboxylate ligands that leads to network interpenetration. However, it turns out that interpenetration is responsible for the formation of voids that have a specific size and shape and are covered with functionalities that selectively recognize different anions on the basis of their dimensions and their preference for specific noncovalent interactions.

## 2. EXPERIMENTAL SECTION

**2.1. Materials and Physical Techniques.** All starting materials, including zinc nitrate hexahydrate, 1,1'-carbonyldiimidazole, 4-aminobenzoic acid, and 4-aminopyridine, were purchased from Aldrich and Merck and used as received. IR spectra were recorded using a Thermo Nicolet IR 100 FT-IR spectrometer. The thermal behavior was measured with a PL-STA 1500 apparatus with a rate of 10 °C min<sup>-1</sup> under a static atmosphere of nitrogen. X-ray powder diffraction (PXRD) measurements were performed using a Philips X'pert diffractometer with monochromated Cu K $\alpha$  radiation. The <sup>1</sup>H NMR spectra were recorded on a Bruker AC-250 MHz spectrometer at ambient temperature in *d*<sub>6</sub>-DMSO. Diffuse reflectance spectroscopy (DRS) and solid-state photoluminescence were performed using an AvaSpec-2048TEC spectrometer. The fluorescence properties in solution were measured at room temperature on a PerkinElmer-L555 fluorescence spectrometer.

**2.2. Synthesis of Ligands.** The 1,3-bis(pyridin-4-yl)urea (L2) ligand was synthesized according to the procedures described in the Supporting Information. Biphenyl-4,4'-dicarboxylic acid (H<sub>2</sub>bpdc) and terephthalic acid (H<sub>2</sub>bdc) were purchased from Aldrich and Merck and used as received.

**2.3. Synthesis of the MOFs TMU-67 and TMU-68.** A DMF solution (15.0 mL) containing Zn(NO<sub>3</sub>)<sub>2</sub>·6H<sub>2</sub>O (0.297 g, 1 mmol), L2 (0.214 g, 1 mmol), and bpdc (0.242 g, 1 mmol) or bdc (0.166 g, 1 mmol) for TMU-67 and TMU-68, respectively, was heated at 100 °C for 72 h in an isothermal oven. After they were cooled to room temperature, the reaction mixtures were filtered and the isolated white crystalline solid was washed with DMF and dried at room temperature. White crystalline solids of [Zn(bpdc)(L2)]·DMF (TMU-67) and [Zn<sub>2</sub>(bdc)<sub>2</sub>(L2)<sub>2</sub>]·2DMF (TMU-68), suitable for X-ray structural analysis, were collected. The compositions of these two compounds were confirmed by single-crystal X-ray structural determinations and TGA. Yields: 64% and 60% for TMU-67 and TMU-68, respectively. FT-IR selected bands for TMU-68 (KBr pellet, cm<sup>-1</sup>): 3355 (w), 1740 (w), 1687 (vs), 1565 (s), 1512 (s), 1380 (m), 1300 (w), 1187 (m), 1021 (w), 850 (w), 785 (w), 531 (w). FT-IR selected bands for TMU-67 (KBr pellet, cm<sup>-1</sup>): 3350 (w), 1737 (w), 1673 (vs), 1578 (vs), 1542 (m), 1513 (m), 1395 (vs), 1308 (m), 1220 (vs), 848 (m), 780 (m), 523 (w). Anal. Found (calcd) for TMU-67: C, 56.72 (56.72); H, 4.24 (4.25), N, 11.48 (11.81). Found (calcd) for TMU-68: C, 51.22 (51.13); H, 4.14 (4.10), N, 13.48 (13.55). Anal. Found (calcd) for activated TMU-67: C, 57.72 (57.76); H, 3.24 (3.49), N, 10.49 (10.78). Found (calcd) for activated TMU-68: C, 51.22 (51.43); H, 3.14 (3.18), N, 12.48 (12.63).

**2.4. Crystal Structure Analysis.** Single-crystal X-ray diffraction data for the metal–organic frameworks TMU-67 and TMU-68 were collected on a Bruker APEX II CCD area detector diffractometer, using graphite-monochromated Mo K $\alpha$  radiation ( $\lambda$  = 0.71073 Å). Data collection was performed at 150 K. A full sphere of reciprocal space was scanned by 0.5°  $\omega$  steps, collecting 1440 frames in four different regions of the reciprocal space. After integration, an empirical absorption correction was made on the basis of the symmetry-equivalent reflection intensities measured.

The structures were solved by direct methods (SIR 2014)<sup>34</sup> and subsequent Fourier synthesis; they were refined by full-matrix least squares on  $F^2$  (SHELX 2014)<sup>35</sup> using all reflections. Weights were assigned to individual observations according to the formula  $w = 1/[\sigma^2(F_o^2) + (aP)^2 + bP]$ , where  $P = (F_o^2 + 2F_c^2)/3$ ;  $a$  and  $b$  were chosen to give a flat analysis of variance in terms of  $F_o^2$ . Anisotropic parameters were assigned to all non-hydrogen atoms (except those of the disordered dimethylformamide molecules in TMU-67). All of the hydrogen atoms were clearly visible in difference-Fourier maps (except those of the disordered dimethylformamide molecules in TMU-67); however, they were eventually placed in idealized positions and refined riding on their parent atom with an isotropic displacement parameter 1.2 (or 1.5) times that of the pertinent parent atom.

In the structure of TMU-67 the solvate dimethylformamide molecule is disordered over two positions, possibly due to the large volume (122 Å<sup>3</sup>) of the cavity occupied. The two overlapping images were refined by applying soft restraints on bond distances and bond angles, on the basis of the mean values obtained from a survey of the Cambridge Structural Database, employing isotropic parameters for all the atoms. Any attempt to refine the solvent molecule employing anisotropic displacement parameters led only to negligible improvements in the  $R$  factors at the expense of a significant increase in the number of refined parameters and in their correlation and were therefore discarded.

The final difference electron density map showed no features of chemical significance, with the largest peaks lying close to the metal atoms.

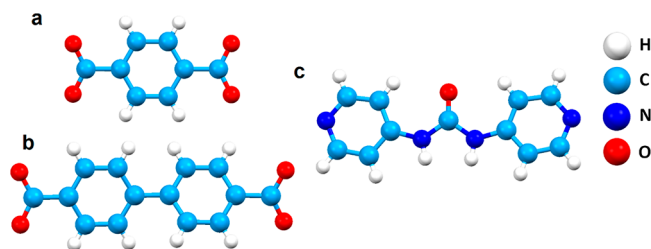
Crystal data, data collection, and refinement details of the structural analyses are summarized in Table S1, while a selection of geometric parameters for the two metal–organic frameworks are collected in Tables S2 and S3.

## 3. RESULTS AND DISCUSSION

**3.1. Structural Description.** TMU-67 and TMU-68 were synthesized under solvothermal conditions by reacting zinc nitrate with the nitrogen-containing pillar ligand 1,3-bis-

(pyridin-4-yl)urea (L2) and, respectively, biphenyl-4,4'-dicarboxylic acid ( $H_2bpd$ c) or terephthalic acid ( $H_2bdc$ ) (Scheme 1).

**Scheme 1.** (a) Terephthalate (bdc), (b) Biphenyl-4,4'-dicarboxylate (bpdc), and (c) 1,3-Bis(pyridin-4-yl)urea (L2) Ligands



A single-crystal X-ray diffraction analysis shows that **TMU-67** crystallizes in the centrosymmetric space group  $P2_1/c$  of the monoclinic crystal system to give a 3-fold interpenetrated 3D framework. The asymmetric unit contains one zinc atom, one L2 pillar ligand, one bpdc carboxylate ligand, and one disordered DMF molecule. Each Zn(II) center is in a distorted-trigonal-bipyramidal environment, coordinating three O atoms (O2, O4<sup>ii</sup>, and O5<sup>iii</sup>) from three different bpdc anions in the equatorial positions and two N atoms (N1 and N4<sup>i</sup>) of two L2 ligands in the axial positions (Figure 1a). One of the two carboxylate groups of the bpdc ligand (O4 and O5) is bridging two metal centers, giving rise to centrosymmetric dimeric units with a Zn...Zn distance of 3.7879(5) Å. These Zn<sub>2</sub>(COO)<sub>2</sub> dimers are further connected to each other

by the  $\kappa^1O$  coordination of the second carboxylate group of the bpdc anion to generate slightly undulating 2D layers of composition [Zn(bpdc)] (Figure 1b). The pillaring of these layers through bridging L2 ligands extends the structure to a translationally (along *c*) 3-fold interpenetrated 3D framework. The topology of a single 3D network can be described as binodal (3,5-*c*) *fet* or as uninodal (6-*c*) *pcu* depending on whether standard or cluster representation procedures were adopted for simplification by the ToposPro program<sup>36</sup> (Figure 2a and Figure S1).

The three interpenetrated 3D networks interact with each other through bifurcated hydrogen bonds involving the uncoordinated oxygen atom of the bpdc ligand and the two NH groups of the urea fragment of L2 ( $N-H\cdots O3 = 2.8847(15)$  and  $2.8222(15)$  Å), while the urea carbonyl group remains free. Each 3D network interacts with the other two to give a single 3D framework (Figure 3a). The removal of DMF molecules from the crystal structure shows the presence of free voids (about 18% of the cell volume), distributed in square-shaped channels running along the crystallographic *c* direction. The walls of these channels are made by phenyl rings of bpdc anions and metal-coordinated oxygen atoms (O2 and O5) of two different carboxylate ligands (Figure 3b).

**TMU-68** crystallizes in the monoclinic  $C2/c$  space group. The asymmetric unit contains one zinc atom, one L2 ligand, two half bdc molecules residing respectively on a 2-fold axis and on a center of inversion, and a DMF molecule (Figure 1d). Similarly to **TMU-67**, each Zn(II) atom adopts a distorted-trigonal-bipyramidal coordination geometry in which the three equatorial positions are occupied by oxygen atoms of three different bdc anions (O2, O3<sup>ii</sup>, and O4) and the two axial

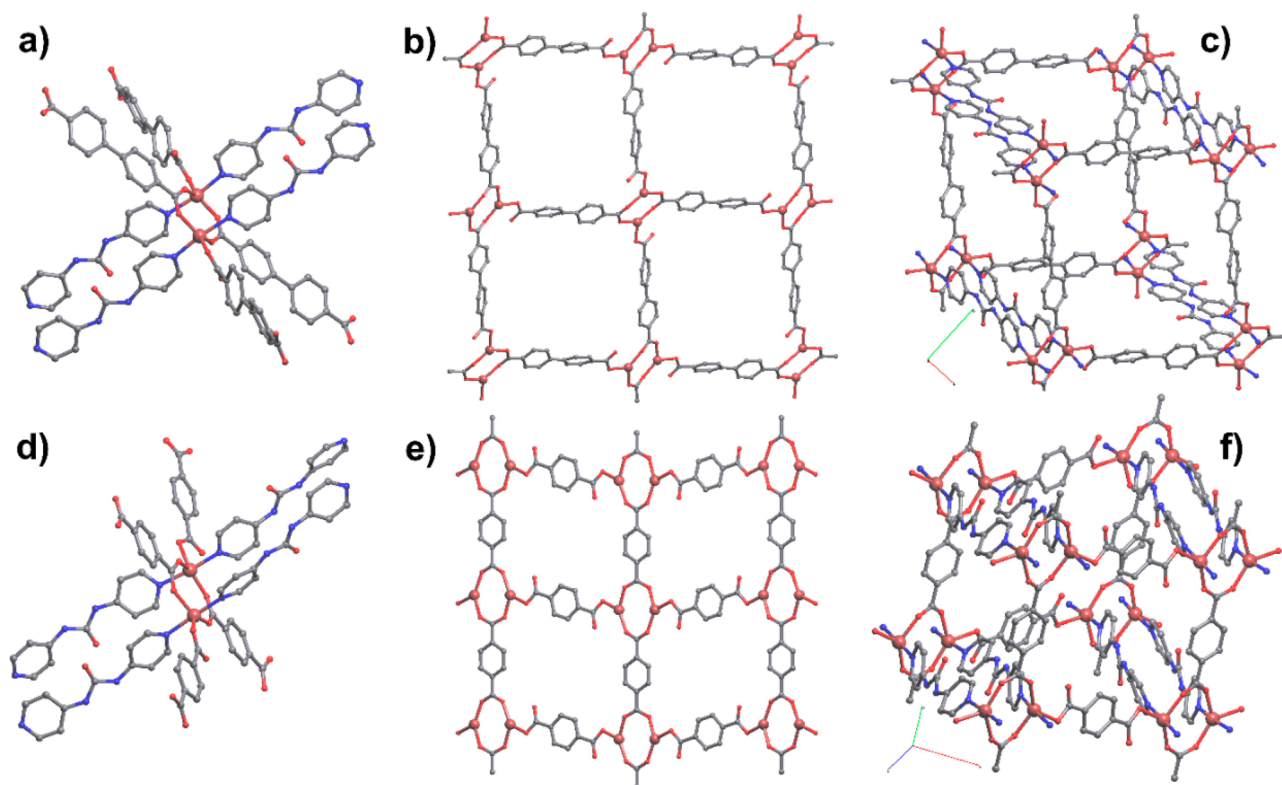


**Figure 1.** Views of the crystal structures of **TMU-67** (in the upper row) and **TMU-68** (in the lower row) showing the dinuclear secondary building units (a, d), the layers composed by zinc dimers and bridging carboxylate ligands (b, e), and portions of single 3D networks showing slightly and strongly distorted cubic cages (c, f). All hydrogen atoms and clathrate solvent molecules are omitted for clarity.

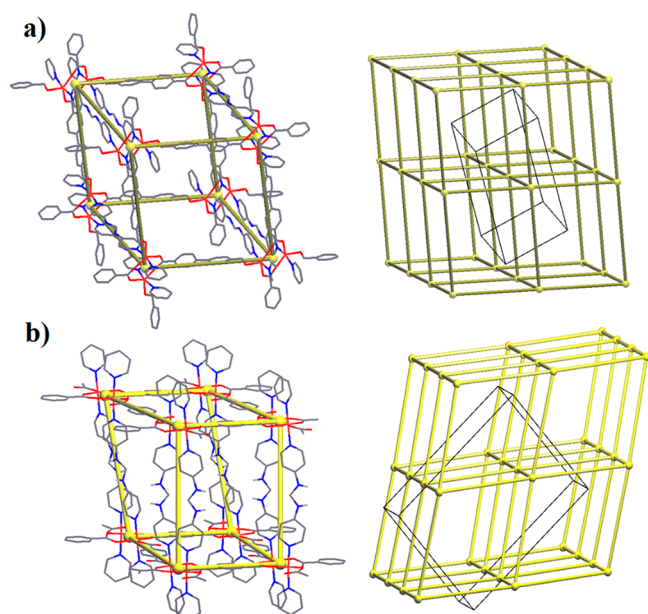


**Figure 2.** TMU-67, represented as a single net in a cluster description as 6-c *pcu* (notice two parallel “double-bridged” edges) (a). TMU-68, represented as a single net in cluster description as 6-c *pcu* (notice four parallel “double-bridged” edges) (b).

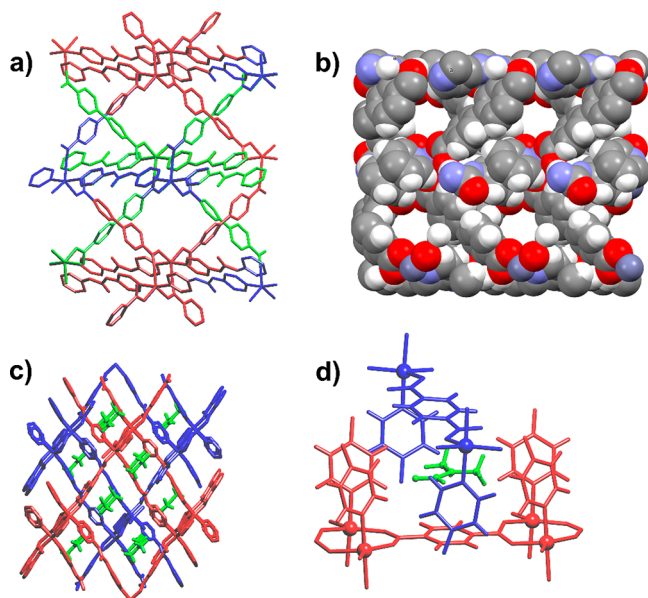


**Figure 3.** Interpenetration in TMU-67 and TMU-68. (a) View along the crystallographic *c* axis of the three interpenetrated networks (showed in three different colors) in TMU-67. (b) Space-filling view along the crystallographic *c* direction of TMU-67 showing monodimensional channels covered by carboxylate oxygen atoms. Clathrate DMF molecule are omitted for clarity. (c) View of TMU-68 along the crystallographic *b* direction showing the 2-fold interpenetrated networks (in blue and red) and clathrate DMF molecules (in green). (d) View of the cavity formed by the interpenetration of two single networks in TMU-68, which is delimited by phenyl rings and occupied by DMF molecules.

positions by nitrogen atoms of two pillaring L2 ligands (N4 in N4<sup>+</sup>). The *bdc* ligand residing on a *C*<sub>2</sub> axis coordinates in a bridging  $\kappa^1\text{O}:\kappa^1\text{O}'$  mode and generates dinuclear [Zn<sub>2</sub>(COO)<sub>2</sub>]<sub>2</sub> units (Zn...Zn = 3.8503(7) Å) similar to

those found in TMU-67. These dimeric units are further connected through centrosymmetric bridging  $\kappa^1\text{O} \text{ bdc}$  groups, giving rise to a flat 2D layer (Figure 1e). All metal centers are then connected through pillaring L2 ligands extending the structure to a translationally 2-fold interpenetrated 3D framework. The topology of the underlying net is binodal 4,5-c *sqc65* or uninodal 6-c *pcu* depending on whether standard or cluster representation procedures are adopted for simplification by the ToposPro program (Figure 2b and Figure S2). Removal of DMF molecules from the crystal structure leaves about 16% of the cell volume as free space. This is distributed in chambers whose walls are made by phenyl rings of both *bdc* and L2 ligands belonging to the two interpenetrated networks, as illustrated in Figure 3d. As was found in TMU-67, also in this case bifurcated hydrogen bonds between NH groups of L2 ligands belonging to one 3D network and uncoordinated oxygen atoms of carboxylic groups belonging to the other interpenetrated 3D network can be recognized (N–H...O5 = 2.760(2) and 2.827(2) Å), giving rise to a single supramolecular framework (Figure 3c). A structural analysis of the two urea-containing frameworks reveals that in both cases, due to interpenetration, the urea groups are not free but are already engaged in hydrogen bonds and are, in principle, not available for anion recognition. On the other hand, the two structures show the presence of free voids which, being distributed differently and exposing different potential recognition sites, have a crucial role in the anion recognition process.

**3.2. MOF Characterization, Anion Sensing, and Selectivity.** TMU-67 and TMU-68 were obtained in good yields as crystalline white solids under identical solvothermal conditions. The purity of these materials was confirmed by a comparison of their X-ray powder diffraction (PXRD) patterns with those calculated from single-crystal XRD data (Figures S3 and S4). Thermogravimetric analysis (TGA) on crystalline samples of as-synthesized TMU-67 and TMU-68 under an atmosphere of N<sub>2</sub> reveals the robustness of the 3D structures, which are stable up to 200 and 170 °C, respectively (Figure S5). The Brunauer–Emmett–Teller (BET) surface areas of TMU-67 and TMU-68 measured with N<sub>2</sub> at 77 K are 224 and 35 m<sup>2</sup> g<sup>−1</sup>, respectively (Figure S6).

It should be noted that, before any application, these materials must be activated in order to expose their functional groups. The trapped solvent can be removed by soaking the crystals in CH<sub>3</sub>CN for 3 days, renewing with fresh CH<sub>3</sub>CN every 24 h, and finally heating the crystals at 100 °C for 24 h. Removal of DMF molecules by this activation procedure was confirmed by FT-IR spectroscopy, in particular by the disappearance of the peaks attributed to DMF (1687 and 1673 cm<sup>−1</sup> for TMU-67 and TMU-68, respectively) in the FT-IR spectra collected on activated samples. Elemental analyses of activated samples also confirmed the removal of solvent molecules.

The incorporation of hydrophilic urea functional groups into the backbone of the two frameworks imparts a hydrophilic character to the materials that makes them suitable platforms for applications in aqueous environments. The hydrophilic character of the two MOFs has been confirmed by performing contact angle measurements of water droplets on the surfaces of TMU-67 and TMU-68, which gave values of 33 and 38°, respectively. The stabilities of the two compounds in water have been also assessed by soaking them in water at room temperature and checking the integrity of the crystal structures

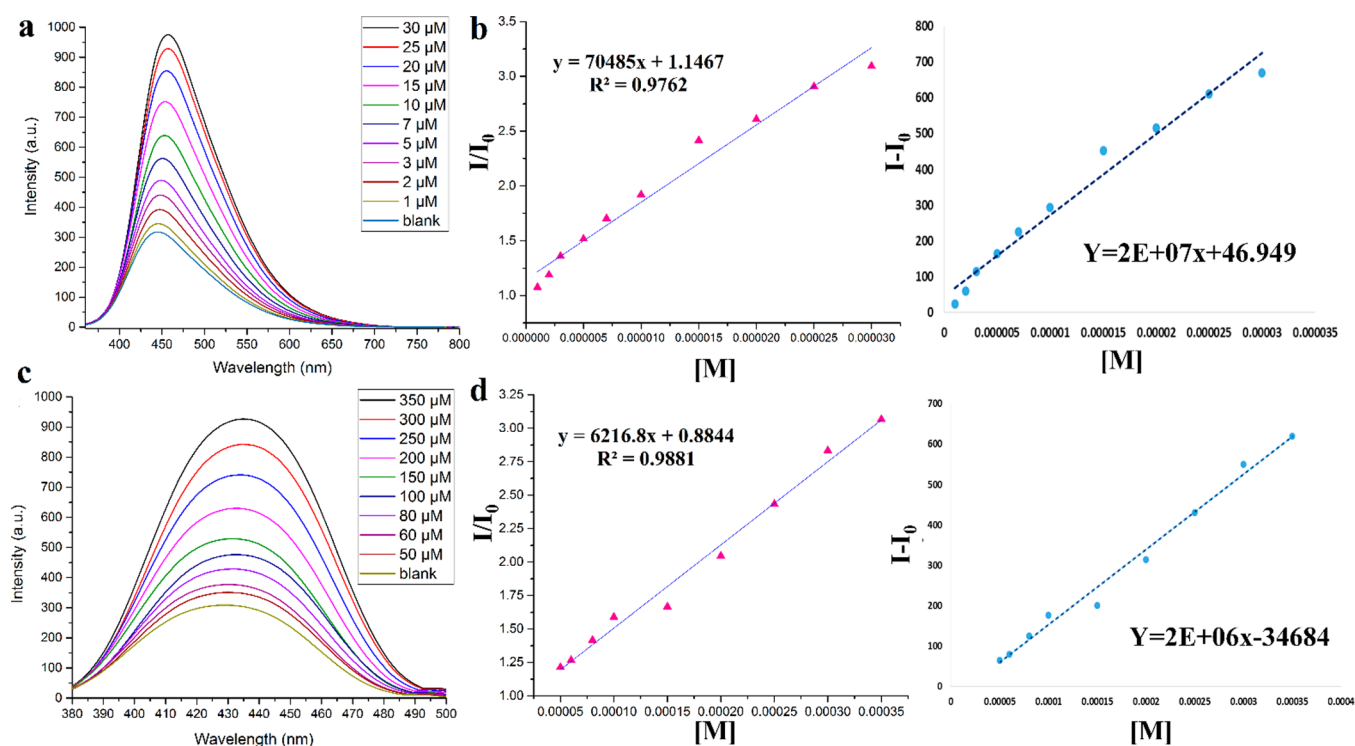


**Figure 4.** Fluorescence emission spectra of (a) TMU-67 and (c) TMU-68 dispersed in aqueous solutions containing the  $\text{H}_2\text{AsO}_4^-$  anion in different concentrations. Corresponding calibration curves for (b) TMU-67 and (d) TMU-68. The limit of detection (LOD) was  $1 \mu\text{M}$  for TMU-67 and  $1 \mu\text{M}$  for TMU-68.

by PXRD. Very small variations in the experimental PXRD patterns collected before and after the soaking confirm the stability of the two MOFs in water and suggest the possibility of employing them for anion sensing in aqueous solutions (Figures S3 and S4).

Metals with a  $d^{10}$  electron configuration are known to be good luminescence centers without unpaired electrons, for which metal to ligand charge transfer (MLCT) transitions are not possible. Due to the combination of rigid aromatic urea-containing organic moieties with  $d^{10}$  Zn(II) centers, TMU-67 and TMU-68 both show an intense ligand-based fluorescence emission. These photoluminescence properties can be exploited to study the anion recognition capabilities of the two MOFs. The two compounds show a broad absorption band centered at 295 nm in the UV–vis spectra and exhibit strong fluorescence at 450 and 430 nm upon excitation at 350 and 370 nm, respectively. To investigate the response of these MOFs toward the loading of different oxoanions and halides, 3 mg of activated crystals of the two compounds was dispersed in 3 mL of aqueous solution containing the sodium salts of anionic analytes and kept at room temperature for 10 min. At the end of the adsorption time, the fluorescence emission spectra of the anion-incorporated MOFs dispersed in aqueous solutions were recorded. Quantitative analysis shows a dramatic fluorescence enhancement proportional to the increase in the anion concentration, particularly for the dihydrogen arsenate loaded TMU-67 framework and for the fluoride loaded TMU-68 framework.

The enhancement of the emission intensity upon anion loading allows ordering the anions on the basis of their affinity for the two MOFs. The order of anion affinity for TMU-67 is  $\text{H}_2\text{AsO}_4^- \gg \text{H}_2\text{PO}_4^- > \text{NO}_2^- > \text{SO}_4^{2-} > \text{HPO}_4^{2-} > \text{NO}_3^- > \text{HAsO}_4^{2-} > \text{ClO}_4^-$ . At the same time, TMU-67 has been found

to be much less sensitive to halides. On the other hand, the order of anion affinity for TMU-68 is  $\text{F}^- \gg \text{H}_2\text{PO}_4^- > \text{Cl}^- > \text{H}_2\text{AsO}_4^- > \text{NO}_2^- > \text{HPO}_4^{2-} > \text{NO}_3^- > \text{HAsO}_4^{2-} > \text{SO}_4^{2-} > \text{ClO}_4^-$ .

In order to quantitatively analyze the relationship between the luminescence intensity of TMU-67 and TMU-68 and the concentration of anions, we defined a luminescence enhancement coefficient  $K_{ec}$  according to the equation  $I/I_0 = 1 + K_{ec}[M]$ , where  $[M]$  is the concentration of the anions,  $I$  represents the luminescence intensity of TMU-67 and TMU-68 suspensions after adding anions up to a specified concentration, and  $I_0$  is the initial luminescence intensity of TMU-67 and TMU-68 suspensions.<sup>37,38</sup> To quantify the enhancing effect exerted by these anions, calibration curves have been constructed by monitoring the fluorescence intensity of TMU-67 and TMU-68 as the concentration of the analytes is varied. The plots of the fluorescence intensity enhancement versus the concentration of  $\text{H}_2\text{AsO}_4^-$  show a reasonable linear correlation, with constant  $K_{ec}$  values of 70485 and  $6217 \text{ M}^{-1}$  for TMU-67 and TMU-68, respectively (Figure 4). The calibration plots for  $\text{H}_2\text{PO}_4^-$  were also found to be linear. However, in this case the measured  $K_{ec}$  values are 16054 and  $8339 \text{ M}^{-1}$  for TMU-67 and TMU-68, respectively (Figures S7 and S11), showing a less pronounced affinity of TMU-67 for the dihydrogen phosphate anion with respect to the dihydrogen arsenate anion. It should be noted that these measurements were carried out at pH 5, so as to make sure that  $\text{H}_2\text{AsO}_4^-$  and  $\text{H}_2\text{PO}_4^-$  were the major species present in solution. On the other hand, TMU-68 shows a high sensitivity to the fluoride anion, with a  $K_{ec}$  value of  $38448 \text{ M}^{-1}$  (Figure S9).

The results of these fluorescence measurements, depicted in Figure 5c, clearly show a preference of TMU-67 for the

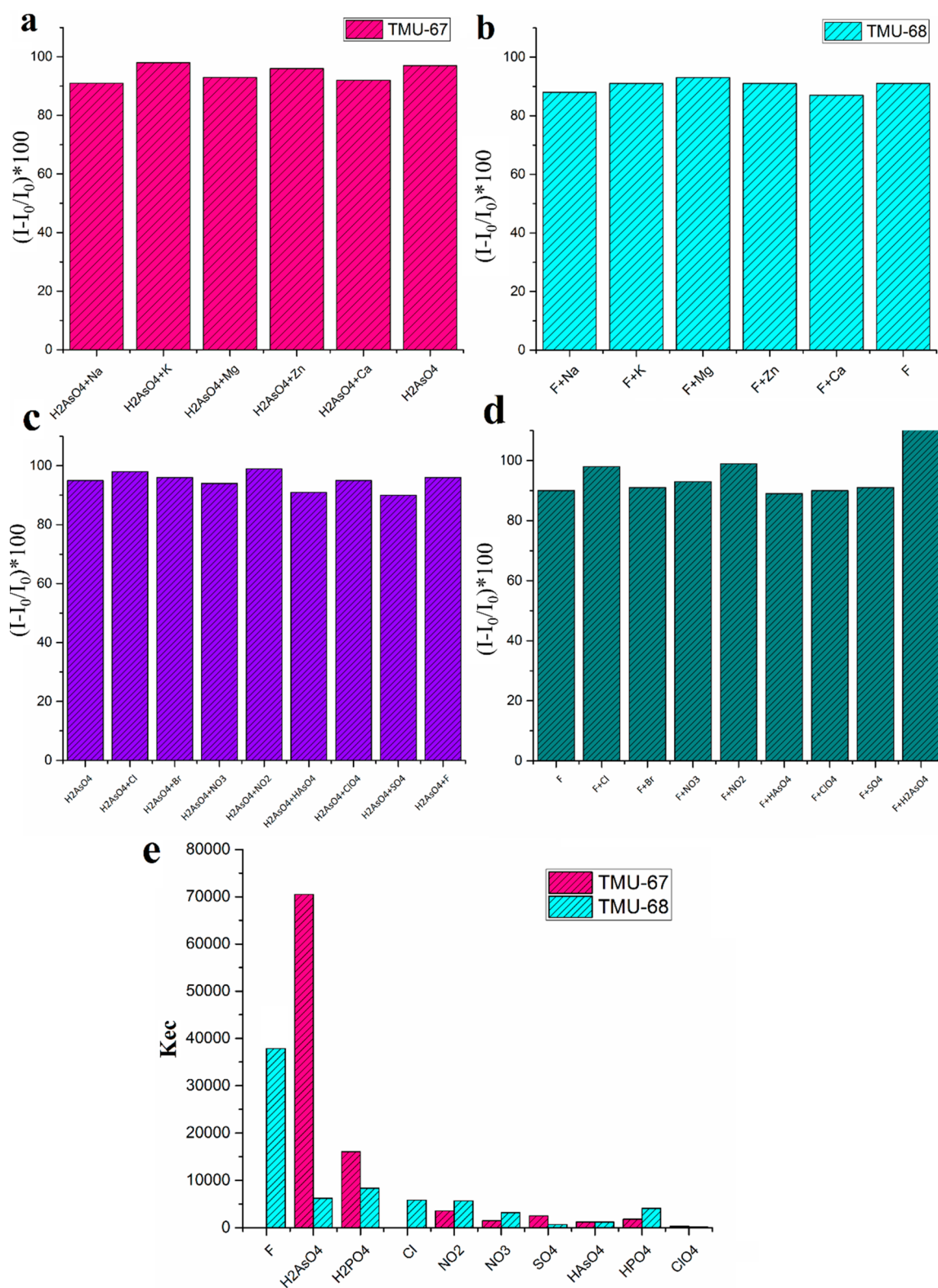


**Figure 5.** Effect of the presence of various possibly interfering cations and anions on the fluorescence enhancement observed for (a, c) TMU-67 in the presence of H<sub>2</sub>AsO<sub>4</sub><sup>−</sup> and for (b, d) TMU-68 in the presence of F<sup>−</sup>. (e) Selectivity of the fluorescence enhancement observed for the two MOFs dispersed in aqueous solution in the presence of different anions, as measured by the corresponding enhancement constants K<sub>ec</sub>.

dihydrogen arsenate anion and, to a lesser extent, the only other oxoanion containing two −OH groups, namely H<sub>2</sub>PO<sub>4</sub><sup>−</sup>, and a preference of TMU-68 for the fluoride anion. In particular, the emission enhancement observed for TMU-67 in the presence of H<sub>2</sub>AsO<sub>4</sub><sup>−</sup> is 4.4 times greater than that

observed in the presence of the quite similar anion H<sub>2</sub>PO<sub>4</sub><sup>−</sup>. If anions that are more diverse (for charge, shape, and presence of H-bond donor groups) are taken into account, the response for the H<sub>2</sub>AsO<sub>4</sub><sup>−</sup> anion is almost 20 times greater. Similar observations can be made for TMU-68 and F<sup>−</sup>, since its

response in the presence of this anion is at least 4.6 times greater than that observed in the presence of other anions. It should be noted that the development of receptors for selective sensing and binding of oxoanions such as  $\text{H}_2\text{AsO}_4^-$  and  $\text{H}_2\text{PO}_4^-$  in the presence of  $\text{F}^-$  is highly desirable and yet still remains a challenge.

To evaluate the possible interference produced by foreign ions in the detection of  $\text{H}_2\text{AsO}_4^-$  by **TMU-67** or of  $\text{F}^-$  by **TMU-68**, fluorescence enhancement was measured in different experiments in which high concentrations of cations (such as  $\text{Na}^+$ ,  $\text{K}^+$ ,  $\text{Mg}^{2+}$ ,  $\text{Ca}^{2+}$  and  $\text{Zn}^{2+}$ ) were added to the solution. Data reported in Figure 5a,b show that the introduction of these possibly interfering cations has a negligible effect (less than a few percent) on the observed response. The interference of other anions on  $\text{H}_2\text{AsO}_4^-$  and  $\text{F}^-$  ions was also investigated. For both ions, most other anions have little interference in the  $\text{H}_2\text{O}$  solution of MOFs (Figure 5c,d). Therefore, the new urea-containing MOFs **TMU-67** and **TMU-68** seem to possess interesting properties of sensitivity and selectivity as receptors for dihydrogen arsenate and fluoride, respectively, even in the presence of competing anions and a variety of possibly interfering cations. In addition, we tested the recycling performance of the sensors. Briefly, **TMU-67** and **TMU-68** were treated with  $\text{F}^-$  and  $\text{H}_2\text{AsO}_4^-$  aqueous solutions again after several times with water. The luminescence enhancement and recovery performance of **TMU-67** and **TMU-68** was repeated for at least three cycles, and the final intensity could still approximately reach the initial value (Figure S14).

PXRD, inductively coupled plasma (ICP) analysis, and atomic absorption spectroscopy (AAS) were used to investigate the stability of the framework employed in the sensing process. While the PXRD pattern indicates the retention of the structure, ICP and AAS analyses reveal almost 0.6–0.8% degradation of the frameworks during the adsorption experiments. Further, the BET values of **TMU-67** and **TMU-68** demonstrated that after three cycles the porosity was essentially the same.

**3.3. Sensing Mechanism.** One of the key challenges in supramolecular chemistry is the synthesis of receptors with convergent sites organized in order to match the functional groups of the guest molecule. These types of receptors show not only high efficiency but also enhanced selectivity in the recognition process, which are considered to be two important requirements for sensing applications. To investigate the possible mechanism for anion recognition by the two MOFs **TMU-67** and **TMU-68**, all of the sites of these frameworks potentially capable of interactions with the anions should be taken into account. Different sites with these characteristics can be found in the structures, in particular (i) the oxygen atoms of the dicarboxylate ligand coordinated to the zinc cations, which are exposed in the main cavities of **TMU-67** (Figure 3b), (ii) the aromatic rings of the bdc and L2 ligands that entirely cover the cavities of **TMU-68** (Figure 3d), and (iii) the N–H bonds of the urea moiety of the ligand L2 that, however, are not exposed on the wall of the cavities of the two structures, since they are involved in hydrogen bonds that bind together the interpenetrated frameworks.

The presence of these sites of interaction nicely accounts for the observed selectivity in the anion recognitions of the two MOFs. Indeed, the exposed oxygen atoms of the dicarboxylate ligands, aligned in couples ( $\text{O}_2$  and  $\text{O}_5^{\text{iii}}$ ; see the Supporting Information for labeling) along the void channels of **TMU-67**,

are correctly oriented and are at a suitable distance (3.121(2) Å) to form a  $R_2^2(8)$  hydrogen bond with a dihydrogen arsenate anion (according to the geometrical parameters found in structures retrieved from the CSD). A similar behavior can be expected for the dihydrogen phosphate anion, the only other species having two OH functionalities, even if the smaller dimensions of this species with respect to the arsenate anion can lead to a less effective interaction.

On the other hand, the role of anion– $\pi$  interactions in sensing fluorides is well-known,<sup>39–41</sup> and the shorter distance between the aromatic rings covering the walls of the voids of **TMU-68** and the center of the cavity (3.662(2) Å) falls in the range reported for these types of interactions. In addition, the voids in the structure of **TMU-68** are partially isolated, being separated by aromatic rings that can allow small species to move between proximate cavities by means of limited libration, in agreement with the selectivity of this MOF for fluoride, the smallest anion of the set employed in this study.

It is interesting to note that the process of anion recognition by the two MOFs can be traced back to the dimension of the voids and the nature of the groups that are covering. These structural features are a result of network interpenetration, a consequence of the tight N–H...O hydrogen bonds between the urea moieties and the dicarboxylate ligands (Figure 6).

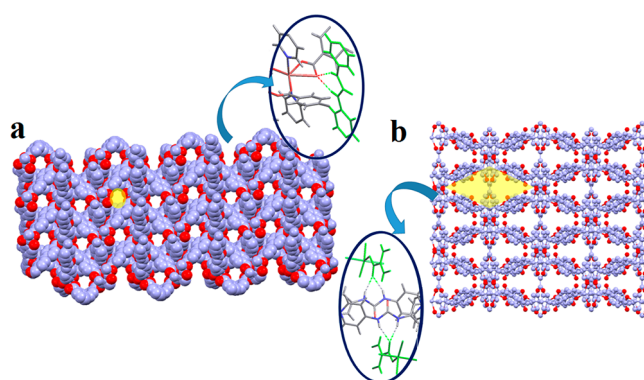


**Figure 6.** Representation of the cavity structures with exposed oxygen atoms (oxygen atoms are shown in red) and the internetwork hydrogen bonding of (a) **TMU-67** and (b) **TMU-68**.

## 4. CONCLUSIONS

There has been an ever-increasing interest in the development of neutral anion receptors for sensing and removal applications in an aqueous environment. Metal–organic frameworks, with their porous and tailorable structures and chemical compositions, are particularly attractive in this context. Of particular interest is the possibility to decorate their porous structures with specific recognition sites, such as hydrogen-bond-donor moieties. For this purpose, in this work we have synthesized and characterized two novel zinc MOFs of mixed dicarboxylate/urea-containing pyridyl ligands, **TMU-67** and **TMU-68**, and their recognition abilities toward different oxo and halide anions in water have been assessed. The two hydrophilic MOFs are stable in water, and their good affinity for anions has been quantified through photoluminescence emission enhancement. The emission enhancement observed for **TMU-67** in the presence of  $\text{H}_2\text{AsO}_4^-$  is 4.4 times greater than that for  $\text{H}_2\text{PO}_4^-$  and almost 20 times greater than that for other anions. Similarly, **TMU-68** gives a response in the presence of  $\text{F}^-$

which is at least 4.6 times greater than that for other anions. Although the urea N–H bonds seem not to play a direct role in the recognition, they are primarily responsible for the process of network interpenetration that in shaping the void creates monodimensional channels, decorated by exposed oxygen atom sites, selective for arsenate sensing in **TMU-67** and isolated cavities, covered by aromatic groups, selective for fluoride sensing in **TMU-68**. As a result, these two new MOFs show an interesting and unexpected selectivity in anion recognition.

## ■ ASSOCIATED CONTENT

### SI Supporting Information

The Supporting Information is available free of charge at <https://pubs.acs.org/doi/10.1021/acs.inorgchem.0c02215>.

Experimental details, crystallographic data, PXRD patterns, TGA and BET experiments, and sensing plots and details (PDF)

## ■ AUTHOR INFORMATION

### Corresponding Authors

**Ali Morsali** – Department of Chemistry, Faculty of Sciences, Tarbiat Modares University, Tehran, Iran; [orcid.org/0000-0002-1828-7287](https://orcid.org/0000-0002-1828-7287); Email: [morsali\\_a@modares.ac.ir](mailto:morsali_a@modares.ac.ir)

**Mao-Lin Hu** – College of Chemistry and Materials Engineering, Wenzhou University, Wenzhou 325035, People's Republic of China; [orcid.org/0000-0003-4130-9859](https://orcid.org/0000-0003-4130-9859); Email: [maolin\\_hu@yahoo.com](mailto:maolin_hu@yahoo.com)

### Authors

**Leili Esrafil** – Department of Chemistry, Faculty of Sciences, Tarbiat Modares University, Tehran, Iran

**Alireza Azhdari Tehrani** – Department of Chemistry, Faculty of Sciences, Tarbiat Modares University, Tehran, Iran; [orcid.org/0000-0001-8070-9164](https://orcid.org/0000-0001-8070-9164)

**Lucia Carlucci** – Dipartimento di Chimica, Università degli Studi di Milano, Milano 20133, Italy; [orcid.org/0000-0001-5856-5280](https://orcid.org/0000-0001-5856-5280)

**Pierluigi Mercandelli** – Dipartimento di Chimica, Università degli Studi di Milano, Milano 20133, Italy; [orcid.org/0000-0002-9473-6734](https://orcid.org/0000-0002-9473-6734)

**Davide M. Proserpio** – Dipartimento di Chimica, Università degli Studi di Milano, Milano 20133, Italy; Samara Center for Theoretical Materials Science (SCTMS), Samara State Technical University, Samara 443100, Russia; [orcid.org/0000-0001-6597-9406](https://orcid.org/0000-0001-6597-9406)

Complete contact information is available at: <https://pubs.acs.org/doi/10.1021/acs.inorgchem.0c02215>

### Notes

The authors declare no competing financial interest.

## ■ ACKNOWLEDGMENTS

We gratefully acknowledge the Tarbiat Modares University, Wenzhou University, and the Università degli Studi di Milano (Piano di Sviluppo d'Ateneo, azione A, PSR2019\_DIP\_005\_Pi\_LCAR) for supporting this research.

## ■ REFERENCES

(1) Steed, J. W. Coordination and organometallic compounds as anion receptors and sensors. *Chem. Soc. Rev.* **2009**, *38*, 506–519.

(2) Gale, P. A. Anion receptor chemistry. *Chem. Commun.* **2011**, *47*, 82–86.

(3) Vilar, R. Anion templates in synthesis and dynamic combinatorial libraries. In *Recognition of Anions*; Springer: 2008; pp 175–206.

(4) Gale, P. A.; Lee, C.-H. Calix [n] pyrroles as Anion and Ion-Pair Complexants. In *Anion Recognition in Supramolecular Chemistry*; Springer: 2010; pp 39–73.

(5) Kumar, R.; Srivastava, A. Anion Binding-Induced White Light Emission using a Water-Tolerant Fluorescent Molecular Tweezer. *Chem. - Eur. J.* **2016**, *22*, 3224–3229.

(6) Pandurangan, K.; Kitchen, J. A.; Blasco, S.; Boyle, E. M.; Fitzpatrick, B.; Feeney, M.; Kruger, P. E.; Gunnlaugsson, T. Unexpected Self-Sorting Self-Assembly Formation of a [4:4] Sulfate: Ligand Cage from a Preorganized Tripodal Urea Ligand. *Angew. Chem.* **2015**, *127*, 4649–4653.

(7) Tepper, R.; Schubert, U. S. Halogen Bonding in Solution: Anion Recognition, Templated Self-Assembly, and Organocatalysis. *Angew. Chem., Int. Ed.* **2018**, *57*, 6004–6016.

(8) Langton, M. J.; Serpell, C. J.; Beer, P. D. Anion recognition in water: recent advances from a supramolecular and macromolecular perspective. *Angew. Chem., Int. Ed.* **2016**, *55*, 1974–1987.

(9) Amendola, V.; Fabbri, L.; Mosca, L. Anion recognition by hydrogen bonding: urea-based receptors. *Chem. Soc. Rev.* **2010**, *39*, 3889–3915.

(10) Busschaert, N.; Caltagirone, C.; Van Rossom, W.; Gale, P. A. Applications of supramolecular anion recognition. *Chem. Rev.* **2015**, *115*, 8038–8155.

(11) Kökçam-Demir, Ü.; Goldman, A.; Esrafil, L.; Gharib, M.; Morsali, A.; Weingart, O.; Janiak, C. Coordinatively unsaturated metal sites (open metal sites) in metal–organic frameworks: design and applications. *Chem. Soc. Rev.* **2020**, *49*, 2751–2798.

(12) Li, J.-R.; Sculley, J.; Zhou, H.-C. Metal–organic frameworks for separations. *Chem. Rev.* **2012**, *112*, 869–932.

(13) Lee, J.; Farha, O. K.; Roberts, J.; Scheidt, K. A.; Nguyen, S. T.; Hupp, J. T. Metal–organic framework materials as catalysts. *Chem. Soc. Rev.* **2009**, *38*, 1450–1459.

(14) Esrafil, L.; Morsali, A.; Dehghani Firuzabadi, F.; Retailleau, P. Development of Porous Cobalt/Copper-doped Carbon Nanohybrids Derived from Functionalized MOF as Efficient Catalysts for the Ullmann Cross-coupling Reaction: Insights into the Active Centers. *ACS Appl. Mater. Interfaces* **2020**, *12*, 43115.

(15) Borissov, A.; Marques, I.; Lim, J. Y.; Félix, V. t.; Smith, M. D.; Beer, P. D. Anion recognition in water by charge-neutral halogen and chalcogen bonding foldamer receptors. *J. Am. Chem. Soc.* **2019**, *141*, 4119–4129.

(16) Azhdari Tehrani, A.; Abbasi, H.; Esrafil, L.; Morsali, A. Urea-containing metal–organic frameworks for carbonyl compounds sensing. *Sens. Actuators, B* **2018**, *256*, 706–710.

(17) Azhdari Tehrani, A.; Esrafil, L.; Abedi, S.; Morsali, A.; Carlucci, L.; Proserpio, D. M.; Wang, J.; Junk, P. C.; Liu, T. Urea metal–organic frameworks for nitro-substituted compounds sensing. *Inorg. Chem.* **2017**, *56*, 1446–1454.

(18) Yao, S.-L.; Zheng, T.-F.; Tian, X.-M.; Liu, S.-J.; Cao, C.; Zhu, Z.-H.; Chen, Y.-Q.; Chen, J.-L.; Wen, H.-R. Dicarboxylate-induced structural diversity of luminescent Zn II/Cd II coordination polymers derived from V-shaped bis-benzimidazole. *CrystEngComm* **2018**, *20*, 5822–5832.

(19) Burtch, N. C.; Jasuja, H.; Walton, K. S. Water stability and adsorption in metal–organic frameworks. *Chem. Rev.* **2014**, *114*, 10575–10612.

(20) Horcajada, P.; Chalati, T.; Serre, C.; Gillet, B.; Sebrie, C.; Baati, T.; Eubank, J. F.; Heurtaux, D.; Clayette, P.; Kreuz, C.; et al. Porous metal–organic-framework nanoscale carriers as a potential platform for drug delivery and imaging. *Nat. Mater.* **2010**, *9*, 172–178.

(21) Khutia, A.; Rammelberg, H. U.; Schmidt, T.; Henninger, S.; Janiak, C. Water sorption cycle measurements on functionalized MIL-101Cr for heat transformation application. *Chem. Mater.* **2013**, *25*, 790–798.

(22) Huang, X.-X.; Qiu, L.-G.; Zhang, W.; Yuan, Y.-P.; Jiang, X.; Xie, A.-J.; Shen, Y.-H.; Zhu, J.-F. Hierarchically mesostructured MIL-101 metal–organic frameworks: supramolecular template-directed synthesis and accelerated adsorption kinetics for dye removal. *CrystEngComm* **2012**, *14*, 1613–1617.

(23) Howarth, A. J.; Wang, T. C.; Al-Juaid, S. S.; Aziz, S. G.; Hupp, J. T.; Farha, O. K. Efficient extraction of sulfate from water using a Zr-metal–organic framework. *Dalton Trans.* **2016**, *45*, 93–97.

(24) Ma, J.-P.; Yu, Y.; Dong, Y.-B. Fluorene-based Cu(II)-MOF: a visual colorimetric anion sensor and separator based on an anion-exchange approach. *Chem. Commun.* **2012**, *48*, 2946–2948.

(25) Shi, P.-F.; Hu, H.-C.; Zhang, Z.-Y.; Xiong, G.; Zhao, B. Heterometal–organic frameworks as highly sensitive and highly selective luminescent probes to detect I<sup>−</sup> ions in aqueous solutions. *Chem. Commun.* **2015**, *51*, 3985–3988.

(26) Kim, K. Entering the recognition domain. *Nat. Chem.* **2009**, *1*, 603–604.

(27) Karmakar, A.; Kumar, N.; Samanta, P.; Desai, A. V.; Ghosh, S. K. A Post-Synthetically Modified MOF for Selective and Sensitive Aqueous-Phase Detection of Highly Toxic Cyanide Ions. *Chem. - Eur. J.* **2016**, *22*, 864–868.

(28) Roberts, J. M.; Fini, B. M.; Sarjeant, A. A.; Farha, O. K.; Hupp, J. T.; Scheidt, K. A. Urea metal–organic frameworks as effective and size-selective hydrogen-bond catalysis. *J. Am. Chem. Soc.* **2012**, *134*, 3334–3337.

(29) Tehrani, A. A.; Abedi, S.; Morsali, A.; Wang, J.; Junk, P. C. Urea-containing metal-organic frameworks as heterogeneous organocatalysts. *J. Mater. Chem. A* **2015**, *3*, 20408–20415.

(30) Alegre-Requena, J. V.; Marqués-López, E.; Herrera, R. P.; Díaz, D. D. Metal–organic frameworks (MOFs) bring new life to hydrogen-bonding organocatalysts in confined spaces. *CrystEngComm* **2016**, *18*, 3985–3995.

(31) Zhang, X.; Zhang, Z.; Boissonnault, J.; Cohen, S. M. Design and synthesis of squaramide-based MOFs as efficient MOF-supported hydrogen-bonding organocatalysts. *Chem. Commun.* **2016**, *52*, 8585–8588.

(32) Antonisse, M. M.; Reinhoudt, D. N. Neutral anion receptors: design and application. *Chem. Commun.* **1998**, 443–448.

(33) Boer, S. A.; Foyle, E. M.; Thomas, C. M.; White, N. G. Anion coordination chemistry using O–H groups. *Chem. Soc. Rev.* **2019**, *48*, 2596–2614.

(34) Burla, M. C.; Caliandro, R.; Carrozzini, B.; Cascarano, G. L.; Cuocci, C.; Giacovazzo, C.; Mallamo, M.; Mazzone, A.; Polidori, G. Crystal structure determination and refinement via SIR2014. *J. Appl. Crystallogr.* **2015**, *48*, 306–309.

(35) Sheldrick, G. M. Crystal structure refinement with SHELXL. *Acta Crystallogr., Sect. C: Struct. Chem.* **2015**, *71*, 3–8.

(36) Blatov, V. A.; Shevchenko, A. P.; Proserpio, D. M. Applied topological analysis of crystal structures with the program package ToposPro. *Cryst. Growth Des.* **2014**, *14*, 3576–3586.

(37) Goswami, R.; Mandal, S. C.; Seal, N.; Pathak, B.; Neogi, S. Antibiotic-triggered reversible luminescence switching in amine-grafted mixed-linker MOF: exceptional turn-on and ultrafast nanomolar detection of sulfadiazine and adenosine monophosphate with molecular keypad lock functionality. *J. Mater. Chem. A* **2019**, *7*, 19471–19484.

(38) Wang, M.; Guo, L.; Cao, D. Amino-Functionalized Luminescent Metal–Organic Framework Test Paper for Rapid and Selective Sensing of SO<sub>2</sub> Gas and Its Derivatives by Luminescence Turn-On Effect. *Anal. Chem.* **2018**, *90*, 3608–3614.

(39) Schottel, B. L.; Chifotides, H. T.; Dunbar, K. R. Anion- $\pi$  interactions. *Chem. Soc. Rev.* **2008**, *37*, 68–83.

(40) Chifotides, H. T.; Dunbar, K. R. Anion- $\pi$  interactions in supramolecular architectures. *Acc. Chem. Res.* **2013**, *46*, 894–906.

(41) Guha, S.; Saha, S. Fluoride ion sensing by an anion- $\pi$  interaction. *J. Am. Chem. Soc.* **2010**, *132*, 17674–17677.